Published in final edited form as:
Cancer Res. 2013 January 15; 73(2): 930–941. doi:10.1158/0008-5472.CAN-12-1389.

Convergence of the ZMIZ1 and NOTCH1 pathways at C-MYC in acute T lymphoblastic leukemias

Lesley A. Rakowski[1], **Derek D. Garagiola**[1], **Choi M. Li**[1], **Margaret Decker**[1], **Sarah Caruso**[1], **Morgan Jones**[2], **Rork Kuick**[3], **Tomasz Cierpicki**[4], **Ivan Maillard**[1,2,3], and **Mark Y. Chiang**[1,3]

[1]Division of Hematology-Oncology, Department of Medicine, University of Michigan School of Medicine, Ann Arbor, MI

[2]Life Sciences Institute, Ann Arbor, MI

[3]University of Michigan Comprehensive Cancer Center, Ann Arbor, MI

[4]Department of Pathology, University of Michigan School of Medicine, Ann Arbor, MI

Abstract

Activating *NOTCH1* mutations are found in 50–60% of human T-cell acute lymphoblastic leukemia (T-ALL) samples. In mouse models, these mutations generally fail to induce leukemia. This observation suggests that NOTCH1 activation must collaborate with other genetic events. Mutagenesis screens previously implicated ZMIZ1 as a possible NOTCH1 collaborator in leukemia. ZMIZ1 is a transcriptional co-activator of the Protein Inhibitor of Activated STAT (PIAS)-like family. Its role in oncogenesis is unknown. Here we show that activated NOTCH1 and ZMIZ1 collaborate to induce T-ALL in mice. ZMIZ1 and activated NOTCH1 are co-expressed in a subset of human T-ALL patients and cell lines. ZMIZ1 inhibition slowed growth and sensitized leukemic cells to corticosteroids and NOTCH inhibitors. Gene expression profiling identified C-MYC, but not other NOTCH-regulated genes, as an essential downstream target of ZMIZ1. ZMIZ1 functionally interacts with NOTCH1 to promote C-MYC transcription and activity. The mechanism does not involve the NOTCH pathway and appears to be indirect and mediated independently of canonical PIAS functions through a novel N-terminal domain. Our study demonstrates the importance of identifying genetic collaborations between parallel leukemic pathways that may be therapeutically targeted. They also raise new inquiries into potential NOTCH-ZMIZ1 collaboration in a variety of C-MYC-driven cancers.

Introduction

Supraphysiological levels of NOTCH signaling have been implicated in a wide variety of cancers including breast cancer, chronic lymphocytic leukemia, T-cell acute lymphoblastic leukemia (T-ALL) and many others (reviewed in(1)). Normally, NOTCH receptors reside at the cell membrane in an inactive state (reviewed in(2)). NOTCH signaling is restrained by the negative regulatory region (NRR), which consists of the Lin-12/Notch repeats (LNR) domain and the heterodimerization domain (HD). NOTCH becomes activated once it engages ligand. γ-secretase cleaves NOTCH, which releases the intracellular domain of NOTCH (ICN). γ-secretase inhibitors (GSIs) are compounds that inhibit this cleavage step. ICN translocates to the nucleus where it engages the CSL/RBP-Jκ DNA binding factor. ICN

Corresponding Author. Mark Y. Chiang, Room 2043, BSRB, 109 Zina Pitcher Place, Ann Arbor, MI 48109-2200, Tel: 734-615-7513, markchia@umich.edu.

The authors have no conflicts of interest to disclose.

is quickly targeted for proteosomal degradation by multiple “degron” signals in its C-terminal PEST domain(3–6).

In T-ALL, NOTCH1 is constitutively activated through mutations in the HD and PEST domains in about 50–60% of patient samples(7). HD domain mutations destabilize the NRR and trigger ligand-independent activation(8, 9). PEST domain mutations remove C-terminal degron sequences, which enhances ICN stability. In mouse models, most leukemia-associated *NOTCH1* mutations cannot initiate T-ALL(10). However, diverse human T-ALL-associated oncogenes such as *TAL1/SCL* and *LMO2* collaborate with Notch1 mutations to induce leukemia in mouse models (reviewed in(11)). In addition, murine retroviral insertional mutagenesis screens identified dominant-negative Ikaros isoforms as NOTCH1 collaborators(12–14). Alterations in IKAROS have been reported in human T-ALL(13–15). In recent mutagenesis screens, leukemia samples with insertions that activated Notch1 frequently had insertions in the 5′ region upstream of the *Zmiz1* gene that led to overexpression of Zmiz1 without disrupting the coding sequence(16–18).

ZMIZ1 (also known as ZIMP10 or RAI17) is a transcriptional co-activator that is related to Protein Inhibitor of Activated STAT (PIAS) family members. PIAS proteins bind and regulate transcription factors such as NF-κB, STAT, and SMAD (reviewed in(19)). Like PIAS members, ZMIZ1 has a highly conserved MIZ (Msx-Interacting Zinc finger) domain that is important for protein-protein interactions and sumoylation(20, 21). ZMIZ1 has a strong transcriptional activation domain and regulates the activity of diverse group transcription factors including the androgen receptor, SMAD3, and p53(20, 22, 23). Mice deficient in Zmiz1 die at embryonic day 10.5 apparently from impaired vasculogenesis(24). Inhibition of ZMIZ1 impaired the growth of a human prostate cancer cell line(25). The N-terminal portion of ZMIZ1 was discovered as a fusion partner of ABL in a single case of Ph-negative ALL(26).

In the present study, we investigated the role of ZMIZ1 in T-ALL induction and maintenance. We show that ectopic NOTCH1 and ZMIZ1 expression cooperated to induce TALL in mice. ZMIZ1 was expressed in a subset of human primary T-ALL samples and cell lines. Inhibition of ZMIZ1 impaired cell growth and sensitized cells to NOTCH inhibitors and glucocorticoids. Mechanistic studies suggested that ZMIZ1 contributes to oncogenesis by indirectly inducing C-MYC through a unique MIZ-independent mechanism.

Materials and Methods

Mice

4–8 week old C57BL/6 mice and NOD-SCID γ-chain deficient mice were obtained from Taconic. All mice were housed in specific pathogen-free facilities at the University of Pennsylvania and the University of Michigan. Experiments were performed according to guidelines from the National Institutes of Health with approved protocols from the Institutional Animal Care and Use Committees at the University of Pennsylvania (Permit #466100) and the University of Michigan (Permit #10298).

Cell lines

HPB-ALL, PF382, and JURKAT were obtained from Jon Aster (Brigham and Women’s Hospital; September, 2004). ALL-SIL, DND41, LOUCY, SKW-3, MOLT-3, THP-6, TALL1, and RPMI8402 were obtained from Andrew Weng (Terry Fox Laboratory). The CEM cell line was obtained from Katherine Collins (University of Michigan; November, 2010). 8946 was obtained from Warren Pear (University of Pennsylvania; September, 2007) and maintained as previously described(27). These cells were tested for C-MYC dependence in the presence of doxycycline monthly. All cell lines were cultured less than six months

after resuscitation, maintained as previously described(7), authenticated using the VNTR PCR assay, and tested for contaminants using MycoAlert (Lonza) every three months.

Antibodies

Flow cytometry antibodies were as follows: CD4 (RM4-5), CD8 (53-6.7); LNGFR (ME20.4-1.H4), CD1 (HI149), CD5 (L17F12), CD7 (4H9), CD8 (RPA-T8), CD11b (ICRF44), CD13 (WM15), CD33 (HIM-34), CD34 (4H-11), CD45 (HI-30), CD117 (104D2), and HLA-DR (L243). Antibodies used for Western blotting are as follows: cleaved Notch1 (V1744, Cell Signaling Technology); ZMIZ1 (RB1963, Abgent); and C-MYC (N-262, Santa Cruz Biotechnology).

Human T-ALL samples

This study was approved by the University of Michigan Institutional Review Board (Permit #HUM00049758). Frozen samples of T-ALL cells were obtained from the University of Pennsylvania, Mignon Loh and the Children's Oncology Group, Linda Holmfeldt and Charles Mulligan.

Gene expression profiling

We used Affymetrix human HG_U133_plus_2 arrays to assay quadruplicate samples of the CEM cell line transduced with ZMIZ1 shRNA as well as control shRNA for 72 hours in the absence of puromycin. The array data have been deposited in NCBI's Gene Expression Omnibus (GEO) as series GSE32523. We collapsed our 3980 differentially expressed probe sets (with $p<0.01$, and fold-change at least 1.3 fold) to 1930 distinct genes increased with ZMIZ1 knockdown, and 935 decreased genes. Our up and down gene lists were separately tested for over-representation in MYC-related curated gene sets from version 3 of MSigDB, using one-sided Fisher Exact tests.

Quantitative real time PCR (qPCR)

Mouse Deltex1 (Mm00492297_m1), CD25 (Mm00434261_m1), Hes1 (Mm00468601_m1) and c-Myc (Mm00487803_m1) were obtained from Applied Biosystems. Sybr green primer sequences are shown in Table S1. All target gene expression values were normalized to normalized to 18S RNA.

Statistical analysis

Linear regression analysis, ANOVA, T-test, and survival curves were performed using Prism. Unless otherwise indicated, p-values were derived from two sample T-tests and values are shown as means ± standard deviation.

Results

ZMIZ1 cooperates with NOTCH1 to induce T-ALL

Murine insertional mutagenesis studies previously suggested that activated Notch1 and Zmiz1 cooperate to induce T-ALL(16–18). To test this possibility, we cloned ZMIZ1 into the retroviral NGFR vector, which expresses ZMIZ1 and a truncated Nerve Growth Factor Receptor (NGFR). "L1601P" is a common leukemia-associated mutation in the HD domain of NOTCH1. "ΔP" is a PEST domain mutation found in the ALL-SIL T-ALL cell line that deletes amino acids 2473–2555. "L1601PΔP" signifies the mutations L1601P and ΔP in cis. L1601PΔP rarely induces leukemia in mice(10). L1601PΔP was cloned into the retroviral GFP vector, which expresses L1601PΔP and green fluorescent protein (GFP). NGFR, ZMIZ1 and L1601PΔP retroviruses, normalized to equal titers among all conditions, were transduced into adult murine BM progenitors (Figure S1A–B). These progenitors were then

transplanted into lethally irradiated mice. Mice expressing L1601PΔP alone transiently generated circulating $CD4^+CD8^+$ double positive (DP) T-cells as previously described ((10) and Figure 1A). In contrast, mice expressing both ZMIZ1 and L1601PΔP developed a sustained rise in aberrant DP T-cells (Figure 1B). None of the control, ZMIZ1, or L1601PΔP mice developed T-ALL (Figure 1C). In contrast, mice expressing both ZMIZ1 and L1601PΔP developed T-ALL with a penetrance of ~60% at 126 days after transplant. The leukemia resembled the previously described T-ALL induced by strong *NOTCH1* alleles with infiltration of the BM, spleen, lymph node, and thymus with leukemic DP T-cells (Figure 1D)(10). Aberrant DP T-cells were not found in the GFP^-NGFR^- compartment (Figure 1D, bottom row).

ZMIZ1 is expressed in a subset of primary human T-ALL samples

To begin determining the relevance of ZMIZ1 to human T-ALL, we screened 14 T-ALL cell lines for ZMIZ1 expression. CEM and T6E cells expressed ZMIZ1 protein (Figure 2A). Protein in several lines was not detectable; RNA was detected, but at levels five fold less or lower compared to cell lines expressing ZMIZ1 protein (data not shown). ETP-ALL is a novel high-risk pediatric T-ALL identified by Coustan-Smith and colleagues at the St. Judes Children's Hospital(28). Homminga and colleagues found that many ETP-ALL samples overexpressed MEF2C(29). The mean RNA expression of ZMIZ1 was ~2.1-fold higher ($p=4\times10^{-8}$) in ETP-ALL than typical T-ALL samples in the Coustan-Smith data set (Figure S2A) and ~2.4-fold higher ($p=8\times10^{-9}$) in the Homminga data set (Figure S2B). We obtained 12 pediatric ETP-ALL and 12 pediatric non-ETP (i.e. "typical") T-ALL RNA samples from the St. Judes Children's Hospital and the Children's Oncology Group. We obtained 15 adult T-ALL samples from the University of Pennsylvania. Mean ZMIZ1 RNA expression was ~22% higher in ETP-ALL than typical T-ALL samples, although not statistically significant (Figure 2B). ZMIZ1 was significantly more highly expressed in the $MEF2C^{hi}$ subset than the $MEF2C^{lo}$ subset of ETP-ALLs (Figure 2C). Like activated NOTCH, ZMIZ1 is expressed in diverse "oncogenetic" clusters besides ETP-ALLs (Figure S2C). ZMIZ1 protein was detected in one ETP-ALL sample (#7), two typical T-ALL samples (#5 and #11) and three adult T-ALL samples (#498, #711, and #790) (Figure 2D). Activated NOTCH1 was detected in five of the six samples that expressed ZMIZ1.

ZMIZ1 is differentially expressed during thymopoiesis

Human T-cell development begins at the ETP/DN1 cell stage and progresses in orderly fashion through immature stages -- DN2, DN3, Immature Single Positive (ISP), $CD3^-$ DP, $CD3^+$ DP – before developing into the mature CD4 and CD8 cells. We analyzed expression of ZMIZ1 in the Dik et al. data set(30). ZMIZ1 was highest in $CD34^+$ cord blood and ETP/DN1 cell stages and decreased with maturation (Figure S2D). We then sorted the analogous subpopulations from murine thymus and LSK cells ($Lineage^-Sca\text{-}1^+Kit^+$) from bone marrow (Figure 2E). The LSK subset contains hematopoietic stem cells and multipotent progenitor cells. Similar to humans, the expression of mouse Zmiz1 was highest in the most primitive thymocyte fractions and significantly decreased with maturation (Figure 2E). Zmiz1 expression spanned approximately 5-fold (Figure 2E). In contrast, ZMIZ1 expression in human T-ALL samples spanned approximately 1000-fold (Figure 2B).

Inhibition of ZMIZ1 function impacts T-ALL proliferation, survival, and metabolism

We transduced CEM and T6E cells with multiple ZMIZ1 shRNA and verified knockdown of RNA and protein (Figure S3A–D). CEM cells transduced with ZMIZ1-silencing shRNA were ~92% fewer than controls after 9 days of growth (Figure 3A). T6E cells transduced with ZMIZ1-silencing shRNA were ~75% fewer than controls (Figure 3B). For our next experiments we used the CEM cell line because it is derived from a human T-ALL and because the effect of ZMIZ1-silencing was relatively strong. ZMIZ1 knockdown delayed

tumor growth by 7–18 days compared to controls after xenotransplantation (Figure 3C–D). ZMIZ1 silencing significantly increased apoptosis by 7-AAD or Annexin V staining (Figure 3E–F, Figure S4A–B). ZMIZ1 knockdown slowed cell cycle progression at the G1-S checkpoint (Figure 3G–H). ZMIZ1 knockdown produced supernatant with a higher pH (Figure S4C). The ZMIZ1-silenced cells were smaller (Figure S4D). After normalizing for effects on cell number, ZMIZ1 inhibition significantly reduced NH_4^+ production (Figure 3I), lactic acid production (Figure 3J), glutamine consumption (Figure S4E), and glucose consumption (Figure S4F). ZMIZ1 inhibition had no effect on differentiation state (Figure S4G). These studies suggest that ZMIZ1 stimulates cell growth through multiple mechanisms.

ZMIZ1 regulates the C-MYC pathway

We next sought to determine the ZMIZ1-regulated gene set. We transduced CEM cells with nonsilencing shRNA control or ZMIZ1-silencing shRNA and performed gene expression profiling. We compared expression values of selected probe sets giving p-values less than 0.01 and average fold-changes of at least 1.3 fold, which selected 3980 probe sets as differentially expressed (2611 up, 1369 down). An identical analysis of the 34 different data sets that can be obtained by permuting the sample labels without giving back the original data gave an average of 35.9 qualifying probe sets, so that we expect less than 1% of our 3980 selected probe sets to be false positives. A subset of these probe sets that satisfied more stringent selection criteria is shown in Figure 4A. ZMIZ1 knockdown repressed C-MYC expression by roughly 70–80% (Figure 4B–C) as early as 48 hours after ZMIZ1 knockdown (Figure S5A–B). Primary and mature (spliced) C-MYC transcripts were similarly reduced (Figure S5C–D). We performed enrichment analysis of the effect of ZMIZ1 knockdown on the sixteen curated gene sets involving C-MYC in the Molecular Signatures Database (Table S2). The genes that decreased upon ZMIZ1 knockdown were significantly enriched in several lists of genes that increased with MYC overexpression. Conversely, the genes that increased with ZMIZ1 knockdown were significantly enriched in lists of genes that decreased with MYC overexpression. For example, ZMIZ1 knockdown significantly reduced the expression of C-MYC target genes *CCND2* (Cyclin D2), *SLC1A4* (ASCT1), *SLC16A1* (MCT1), *DKC1*, and *ODC1* (Figure 4B–C). Silencing ZMIZ1 with multiple shRNAs reduced C-MYC expression by Western blot (Figure 5A) and qPCR (Figure 5B). These data suggest that ZMIZ1 regulates the expression and activity of C-MYC.

ZMIZ1 cooperates with NOTCH1 to induce the C-MYC pathway

C-*MYC* is a direct target of NOTCH1(31–33). The 8946 cell line is derived from a murine T-ALL driven by an inducible human *C-MYC* transgene. It does not express Zmiz1 (data not shown). 8946 cells die upon doxycycline addition, which represses C-MYC expression, but can be rescued by transduction of strong NOTCH1 alleles that upregulate the expression of endogenous murine *c-Myc*(31). “N1ΔP” is the NOTCH1 allele with the ΔP mutation alone. In terms of NOTCH signal strength, N1ΔP is very weak, L1610P is weak, and L1601PΔP is moderately strong(10). We transduced N1ΔP, L1601P, or L1601PΔP into 8946 cells in combination with either the NGFR vector or ZMIZ1. ZMIZ1 alone failed to rescue 8946 cells after withdrawal of C-MYC (Figure 5C, I). N1ΔP, L1601P, or L1601PΔP alone weakly rescued 8946 cells if at all (Figure 5C, J–L). In contrast, ZMIZ1 strongly enhanced the ability of N1ΔP, L1601P, or L1601PΔP to rescue 8946 cells by 18–36 fold (Figure 5C, J–L). Similarly, ZMIZ1 strongly enhanced the ability of N1ΔP, L1601P, or L1601PΔP to induce expression of *c-Myc* (Figure 5D) and its target gene *Cad* (Figure 5E). These data suggest that ZMIZ1 cooperates with NOTCH1 to induce *C-MYC* transcription and activity.

ZMIZ1 appears to regulate C-MYC indirectly through a novel, MIZ-independent transcriptional mechanism and not through the NOTCH signaling pathway

To further investigate the mechanism of ZMIZ1, we subcloned two 8946 cells that expressed the NGFR control vector and two that expressed ZMIZ1. We turned off C-MYC transcription by adding doxycycline. We did not observe any differences between the rate of loss of C-MYC protein between the ZMIZ1-expressing cells and control cells (Figure S6A). Together with Figure S5C–D, these data suggest that ZMIZ1 does not regulate C-MYC through post-transcriptional mechanisms. ZMIZ1 did not enhance the ability of N1ΔP, L1601P, or L1601PΔP to induce Notch1 target genes (other than *c-Myc*) such as *Dtx1* (Figure 5F), *Il2ra* (Figure 5G), and *Hes1* (Figure 5H). We could not detect association of ZMIZ1 with NOTCH1 using immunoprecipitation assays in three ZMIZ1-expressing cell lines (Figure S6B). Microarray analysis described in Figure 4 showed that ZMIZ1 knockdown did not significantly affect well-established NOTCH1 targets in T-cells such as *DTX1*, *IFI-204, CCR7, LEF1, NOTCH1*, *NOTCH3*, *IL2RA*, *HES1*, *NRARP*, *CCND3,* and *TCF7* (data not shown). These data suggest that ZMIZ1 does not regulate the NOTCH signaling pathway. Chromatin immunoprecipitates did not show association of ZMIZ1 with the ~6 Kb region upstream of the *MYC* transcriptional start site (data not shown). Furthermore, a chimera consisting of ZMIZ1 fused to the ligand-binding domain of the estrogen receptor (ZMIZ1-ER) induced C-MYC RNA at 48 hours (Figure S7A), but not at 6 hours (Figure S7B) after treatment with 4-OHT. These data suggest that the mechanism of ZMIZ1 is likely indirect. Finally, structure-function analysis (Figure 6A) showed that the MIZ domain, but not the N-terminal domain, was dispensable for rescue of 8946 cells after C-MYC withdrawal (Figure 6B) and for induction of c-Myc (Figure 6C). The N-terminal domain has no known function, but appears highly ordered (Figure 6D). These data suggest that ZMIZ1 regulates C-MYC through a novel, MIZ-independent mechanism.

C-MYC is an essential but insufficient effector of ZMIZ1 functions

To determine whether C-MYC can substitute for ZMIZ1, we transduced C-MYC into CEM cells to maintain C-MYC levels irrespective of ZMIZ1 levels (Figure S8A–B). Ectopic expression of C-MYC did not rescue growth of CEM cells in which ZMIZ1 was silenced. QPCR and Western blot confirmed that C-MYC was ectopically expressed (data not shown and Figure S8C). Enforced C-MYC increased apoptosis (Figure S9A–D) in association with a small increase in the G1-S blockade (Figure S9E–F). These data show that C-MYC is not the sole mediator of ZMIZ1 functions. However, it was still possible that C-MYC is required for ZMIZ1 oncogenic functions. To test whether C-MYC is required for CEM growth, we transduced CEM cells with MAD or A-MAX (Figure S8D–E). MAD and A-MAX are dominant-negative inhibitors of C-MYC(31, 34). MAD and A-MAX significantly inhibited growth of CEM cells. Thus, repression of C-MYC, due to knockdown of ZMIZ1, would be expected to impair cell growth. These data suggest that C-MYC is a required, but insufficient effector of ZMIZ1 functions. Knockdown of ZMIZ1 may impair cell growth in part due to reduction of C-MYC levels.

ZMIZ1 silencing sensitizes leukemic cells to NOTCH inhibitors and glucocorticoids

We next determined whether the collaboration between ZMIZ1 and NOTCH could be therapeutically targeted. GSIs are being tested for the treatment of T-ALL(35, 36). THP-6 is a human T-ALL cell line that co-expresses ZMIZ1 and activated NOTCH1 (Figure S10A). CEM and THP-6 cells transduced with control shRNA were fully or partly resistant to GSI (Figure 7A, S10B). However, GSI vs. DMSO growth inhibition was significantly greater in ZMIZ1 shRNA-treated cells than control shRNA-treated cells ($p<0.0001$). In contrast to CEM and THP-6 cells, T6E cells are sensitive to GSI(31). However, under low dose GSI conditions, there was significantly greater GSI vs. DMSO growth inhibition in ZMIZ1 shRNA-treated cells than control shRNA-treated cells (Figure S10C, $p=0.0152$). To test

whether ZMIZ1 inhibition could be added to glucocorticoid therapy given the similarities between the glucocorticoid and androgen receptors, we treated CEM cells with ZMIZ1 shRNA and dexamethasone (Figure 7B). CEM cells transduced with ZMIZ1 shRNA were significantly more sensitive to dexamethasone than controls (Figure 7C). Mifepristone, a glucocorticoid inhibitor, reversed the sensitivity of the CEM cells to glucocorticoids (Figure 7D–E). DND-41 cells do not express ZMIZ1 (Figure 2A). DND-41 cells were equally sensitive to dexamethasone regardless of ZMIZ1 shRNA treatment (Figure 7F–G). These data suggest that ZMIZ1 inhibition may enhance targeting of a subset of T-ALL cells with GSI or glucocorticoids.

Discussion

Activating NOTCH1 mutations can occur prior to the acquisition of other oncogenic events and well in advance of the clinical appearance of T-ALL(37). Some NOTCH1 alleles such as ICN are sufficiently strong to initiate leukemogenesis in mice. In contrast, the vast majority of leukemia-associated NOTCH1 alleles are insufficient(10). This observation suggests that additional genes collaborate with activated NOTCH1 to induce leukemia. Insertional mutagenesis studies in mice identified ZMIZ1 as a possible NOTCH1 collaborator in leukemia development(16–18). Our studies verified that ZMIZ1 collaborates with leukemia-associated NOTCH1 alleles to induce T-ALL in mice. ZMIZ1 is overexpressed in a subset of T-ALL samples. However, like NOTCH1 activation, ZMIZ1 overexpression does not appear to be limited to a specific oncogenetic subset. Indeed, samples that expressed ZMIZ1 frequently expressed activated NOTCH1. Our studies also show that ZMIZ1 may be required for leukemia growth. Together, these findings suggest that ZMIZ1 is an oncogene. It may be a clinically relevant therapeutic target in a subset of T-ALL patients.

In our previous report(10), the penetrance of T-ALL by L1601PΔP in the retroviral transduction/bone marrow transplantation mouse model was ~25%. In the current report, none of the L1601PΔP mice developed T-ALL. The difference between the two reports was viral titer. Our current protocol used four-fold less L1601PΔP virus in order to add the ZMIZ1 virus. This reduction in titer likely explains the difference in penetrance. The dose of NOTCH signaling is critically important for leukemic induction(10). The penetrance of T-ALL of our reports(10) is less than another report by Medyouf et al(38). Our protocol used the C57BL/6 strain in contrast to the C57BL/6 X FvB strain in the Medyouf study. Similar numbers of cells were transferred. Titers and radiation dose may have differed from our protocol, which is detailed in Supplemental Material and Methods.

In addition to Zmiz1, retroviral insertional mutagenesis screens identified Ikaros dominant-negative isoforms and Lunatic Fringe as collaborators of Notch1(16). These genes enhance Notch signaling through a global effect on Notch target genes. In contrast, the collaboration between ZMIZ1 and NOTCH1 appears restricted to just one NOTCH target -- C-MYC. In T-ALL, C-MYC promotes proliferation and glucose/glutamine metabolism(31–33) and can often rescue cell death after withdrawal of NOTCH signaling(31, 39). However, the importance of C-MYC in T-ALL remains to be determined(40). Murine insertional mutagenesis studies showed that insertions in the *Notch1* locus preceded insertions in the *Zmiz1* locus(16). Thus, NOTCH1 activation may predispose cells to recruit ZMIZ1 overexpression in order to amplify the C-MYC signal. The dependence on ZMIZ1 may be an example of synthetic lethality of NOTCH1 activation.

Additional studies will be needed to better characterize the mechanism of ZMIZ1. C-MYC appears to be a required but insufficient effector of ZMIZ1 oncogenic functions. ZMIZ1, like PIAS proteins, may regulate transcription broadly through multiple target genes to

achieve its biological functions. Our data suggests that that C-MYC, combined with additional ZMIZ1 effectors, will drive cell growth. Given the pro-apoptotic functions of C-MYC ((41, 42), Figure S9), we are interrogating our microarray data for effectors that counter apoptosis. We plan to test the ability of these effectors in combination with C-MYC to substitute for ZMIZ1. Additional studies will also be needed to determine how ZMIZ1 collaborates with NOTCH1. ZMIZ1 does not appear to target the NOTCH1 pathway or C-MYC post-transcriptionally. Instead, ZMIZ1 may induce *C-MYC* transcription through indirect mechanisms. ZMIZ1 has no DNA binding domain. It functions by binding transcription factors to enhance their transcriptional activity. PIAS and PIAS-like proteins interact with a broad range of transcription factors through the MIZ domain(19). Therefore, identifying a single direct mechanism by which ZMIZ1 regulates C-MYC may not be straightforward. Furthermore, the MIZ domain, but not the N-terminal domain, appears to be dispensable. The N-terminal domain of ZMIZ1 is not shared with PIAS family members and has no known functions. Therefore, the mechanism of ZMIZ1 appears to be novel and independent of canonical PIAS functions. Solving the mechanism will require proteomic approaches to identify direct binding partners of the N-terminal domain.

NOTCH signaling has been implicated in many cancers. The literature, publically available gene expression data sets, and our own observations in the NCI-60 cell lines suggest that ZMIZ1 is frequently co-expressed with NOTCH in diverse cancers ((25) and data not shown). Thus, it is possible that the collaboration between ZMIZ1 and NOTCH may extend to other cancers besides T-ALL. Targeting the ZMIZ1-NOTCH collaboration may prove to be a general alternative method of targeting C-MYC and other pathways.

Supplementary Material

Refer to Web version on PubMed Central for supplementary material.

Acknowledgments

We thank Jon Aster, Warren Pear, Andrew Weng, Zijie Sun, Thomas Lanigan, Linda Holmfeldt, Charles Mullighan, Dario Campana, Charles Mullighan, Xiaoping Su, Candice Romany, Olga Shestova, Eric Fearon, Mignon Loh and the Children's Oncology Group (COG) for invaluable assistance. We are grateful to Warren Pear, in whose lab these studies were initiated.

Grant support

M.Y.C. –ACS grant (RSG-11-189-01-TBG), V Foundation grant, Alex's Lemonade Stand Award; R.K. -- Comprehensive Cancer Center Core Grant (5 P30 #CA 46592); COG Cell Bank Grant (NIH NCI U24 CA114766) and the COG Clinical Trials Grant (U10 CA98543); M.J. -- NIH predoctoral training grant (5-T32-HD007515); I.M. -- Kimmel Scholar Award (SKF-10-136) and NIH research grant (R01-AI091627).

References

1. Lobry C, Oh P, Aifantis I. Oncogenic and tumor suppressor functions of Notch in cancer: it's NOTCH what you think. Journal of Experimental Medicine. 2011; 208:1931–5. [PubMed: 21948802]
2. Kopan R, Ilagan MX. The canonical Notch signaling pathway: unfolding the activation mechanism. Cell. 2009; 137:216–33. [PubMed: 19379690]
3. Chiang MY, Xu ML, Histen G, Shestova O, Roy M, Nam Y, et al. Identification of a conserved negative regulatory sequence that influences the leukemogenic activity of NOTCH1. Mol Cell Biol. 2006; 26:6261–71. [PubMed: 16880534]
4. O'Neil J, Grim J, Strack P, Rao S, Tibbitts D, Winter C, et al. FBW7 mutations in leukemic cells mediate NOTCH pathway activation and resistance to {gamma}-secretase inhibitors. J Exp Med. 2007; 204:1813–24. [PubMed: 17646409]

5. Thompson BJ, Buonamici S, Sulis ML, Palomero T, Vilimas T, Basso G, et al. The SCFFBW7 ubiquitin ligase complex as a tumor suppressor in T cell leukemia. J Exp Med. 2007; 204:1825–35. [PubMed: 17646408]
6. Fryer CJ, White JB, Jones KA. Mastermind recruits CycC:CDK8 to phosphorylate the Notch ICD and coordinate activation with turnover. Mol Cell. 2004; 16:509–20. [PubMed: 15546612]
7. Weng AP, Ferrando AA, Lee W, Morris JPt, Silverman LB, Sanchez-Irizarry C, et al. Activating mutations of NOTCH1 in human T cell acute lymphoblastic leukemia. Science. 2004; 306:269–71. [PubMed: 15472075]
8. Malecki MJ, Sanchez-Irizarry C, Mitchell JL, Histen G, Xu ML, Aster JC, et al. Leukemia-associated mutations within the NOTCH1 heterodimerization domain fall into at least two distinct mechanistic classes. Mol Cell Biol. 2006; 26:4642–51. [PubMed: 16738328]
9. Gordon WR, Vardar-Ulu D, Histen G, Sanchez-Irizarry C, Aster JC, Blacklow SC. Structural basis for autoinhibition of Notch. Nat Struct Mol Biol. 2007; 14:295–300. [PubMed: 17401372]
10. Chiang MY, Xu L, Shestova O, Histen G, L'Heureux S, Romany C, et al. Leukemia-associated NOTCH1 alleles are weak tumor initiators but accelerate K-ras-initiated leukemia. Journal of Clinical Investigation. 2008; 118:14.
11. Aster JC, Pear WS, Blacklow SC. Notch Signaling in Leukemia. Annu Rev Pathol. 2007; 3:587–613. [PubMed: 18039126]
12. Beverly LJ, Capobianco AJ. Perturbation of Ikaros isoform selection by MLV integration is a cooperative event in Notch(IC)-induced T cell leukemogenesis. Cancer Cell. 2003; 3:551–64. [PubMed: 12842084]
13. Marcais A, Jeannet R, Hernandez L, Soulier J, Sigaux F, Chan S, et al. Genetic inactivation of Ikaros is a rare event in human T-ALL. Leuk Res. 2010; 34:426–9. [PubMed: 19796813]
14. Sun L, Crotty ML, Sensel M, Sather H, Navara C, Nachman J, et al. Expression of dominant-negative Ikaros isoforms in T-cell acute lymphoblastic leukemia. Clin Cancer Res. 1999; 5:2112–20. [PubMed: 10473095]
15. Zhang J, Ding L, Holmfeldt L, Wu G, Heatley SL, Payne-Turner D, et al. The genetic basis of early T-cell precursor acute lymphoblastic leukaemia. Nature. 2012; 481:157–63. [PubMed: 22237106]
16. Uren AG, Kool J, Matentzoglu K, de Ridder J, Mattison J, van Uitert M, et al. Large-scale mutagenesis in p19(ARF)- and p53-deficient mice identifies cancer genes and their collaborative networks. Cell. 2008; 133:727–41. [PubMed: 18485879]
17. Dupuy AJ, Akagi K, Largaespada DA, Copeland NG, Jenkins NA. Mammalian mutagenesis using a highly mobile somatic Sleeping Beauty transposon system. Nature. 2005; 436:221–6. [PubMed: 16015321]
18. Berquam-Vrieze KE, Nannapaneni K, Brett BT, Holmfeldt L, Ma J, Zagorodna O, et al. Cell of origin strongly influences genetic selection in a mouse model of T-ALL. Blood. 2011; 118:4646–56. [PubMed: 21828136]
19. Shuai K, Liu B. Regulation of gene-activation pathways by PIAS proteins in the immune system. Nat Rev Immunol. 2005; 5:593–605. [PubMed: 16056253]
20. Sharma M, Li X, Wang Y, Zarnegar M, Huang CY, Palvimo JJ, et al. hZimp10 is an androgen receptor co-activator and forms a complex with SUMO-1 at replication foci. EMBO Journal. 2003; 22:6101–14. [PubMed: 14609956]
21. Beliakoff J, Sun Z. Zimp7 and Zimp10, two novel PIAS-like proteins, function as androgen receptor coregulators. Nucl Recept Signal. 2006; 4:e017. [PubMed: 16862223]
22. Lee J, Beliakoff J, Sun Z. The novel PIAS-like protein hZimp10 is a transcriptional co-activator of the p53 tumor suppressor. Nucleic Acids Research. 2007; 35:4523–34. [PubMed: 17584785]
23. Li X, Thyssen G, Beliakoff J, Sun Z. The novel PIAS-like protein hZimp10 enhances Smad transcriptional activity. Journal of Biological Chemistry. 2006; 281:23748–56. [PubMed: 16777850]
24. Beliakoff J, Lee J, Ueno H, Aiyer A, Weissman IL, Barsh GS, et al. The PIAS-like protein Zimp10 is essential for embryonic viability and proper vascular development. Molecular & Cellular Biology. 2008; 28:282–92. [PubMed: 17967885]

25. Peng Y, Lee J, Zhu C, Sun Z. A novel role for protein inhibitor of activated STAT (PIAS) proteins in modulating the activity of Zimp7, a novel PIAS-like protein, in androgen receptor-mediated transcription. Journal of Biological Chemistry. 2010; 285:11465–75. [PubMed: 20159969]
26. Soler G, Radford-Weiss I, Ben-Abdelali R, Mahlaoui N, Ponceau JF, Macintyre EA, et al. Fusion of ZMIZ1 to ABL1 in a B-cell acute lymphoblastic leukaemia with a t(9;10)(q34;q22.3) translocation. Leukemia. 2008; 22:1278–80. [PubMed: 18007576]
27. Felsher DW, Bishop JM. Reversible tumorigenesis by MYC in hematopoietic lineages. Mol Cell. 1999; 4:199–207. [PubMed: 10488335]
28. Coustan-Smith E, Mullighan CG, Onciu M, Behm FG, Raimondi SC, Pei D, et al. Early T-cell precursor leukaemia: a subtype of very high-risk acute lymphoblastic leukaemia. Lancet Oncol. 2009; 10:147–56. [PubMed: 19147408]
29. Homminga I, Pieters R, Langerak AW, de Rooi JJ, Stubbs A, Verstegen M, et al. Integrated transcript and genome analyses reveal NKX2-1 and MEF2C as potential oncogenes in T cell acute lymphoblastic leukemia. Cancer Cell. 2011; 19:484–97. [PubMed: 21481790]
30. Dik WA, Pike-Overzet K, Weerkamp F, de Ridder D, de Haas EF, Baert MR, et al. New insights on human T cell development by quantitative T cell receptor gene rearrangement studies and gene expression profiling. Journal of Experimental Medicine. 2005; 201:1715–23. [PubMed: 15928199]
31. Weng AP, Millholland JM, Yashiro-Ohtani Y, Arcangeli ML, Lau A, Wai C, et al. c-Myc is an important direct target of Notch1 in T-cell acute lymphoblastic leukemia/lymphoma. Genes Dev. 2006; 20:2096–109. [PubMed: 16847353]
32. Sharma VM, Calvo JA, Draheim KM, Cunningham LA, Hermance N, Beverly L, et al. Notch1 contributes to mouse T-cell leukemia by directly inducing the expression of c-myc. Mol Cell Biol. 2006; 26:8022–31. [PubMed: 16954387]
33. Palomero T, Barnes KC, Real PJ, Bender JL, Sulis ML, Murty VV, et al. CUTLL1, a novel human T-cell lymphoma cell line with t(7;9) rearrangement, aberrant NOTCH1 activation and high sensitivity to gamma-secretase inhibitors. Leukemia. 2006; 20:1279–87. [PubMed: 16688224]
34. Rishi V, Gal J, Krylov D, Fridriksson J, Boysen MS, Mandrup S, et al. SREBP-1 dimerization specificity maps to both the helix-loop-helix and leucine zipper domains: use of a dominant negative. Journal of Biological Chemistry. 2004; 279:11863–74. [PubMed: 14702347]
35. Deangelo DJ, Stone RM, Silverman LB, Stock W, Attar EC, Fearen I, et al. A phase I clinical trial of the notch inhibitor MK-0752 in patients with T-cell acute lymphoblastic leukemia/lymphoma (T-ALL) and other leukemias. Journal of Clinical Oncology, 2006 ASCO Annual Meeting Proceedings. 2006; 24:6585.
36. Real PJ, Ferrando AA. NOTCH inhibition and glucocorticoid therapy in T-cell acute lymphoblastic leukemia. Leukemia. 2009; 23:1374–7. [PubMed: 19357700]
37. Eguchi-Ishimae M, Eguchi M, Kempski H, Greaves M. NOTCH1 mutation can be an early, prenatal genetic event in T-ALL. Blood. 2008; 111:376–8. [PubMed: 17901244]
38. Medyouf H, Gao X, Armstrong F, Gusscott S, Liu Q, Gedman AL, et al. Acute T-cell leukemias remain dependent on Notch signaling despite PTEN and INK4A/ARF loss. Blood. 2010; 115:1175–84. [PubMed: 20008304]
39. Chiang MY, Childs ME, Romany C, Shestova O, Aster J, Pear WS. C-Myc but not AKT can substitute for Notch in lymphomagenesis. Blood (ASH Annual Meeting Abstracts). 2009:114.
40. Demarest RM, Dahmane N, Capobianco AJ. Notch is oncogenic dominant in T-cell acute lymphoblastic leukemia. Blood. 2011; 117:2901–9. [PubMed: 21217079]
41. Pelengaris S, Rudolph B, Littlewood T. Action of Myc in vivo - proliferation and apoptosis. Curr Opin Genet Dev. 2000; 10:100–5. [PubMed: 10679391]
42. Prendergast GC. Mechanisms of apoptosis by c-Myc. Oncogene. 1999; 18:2967–87. [PubMed: 10378693]

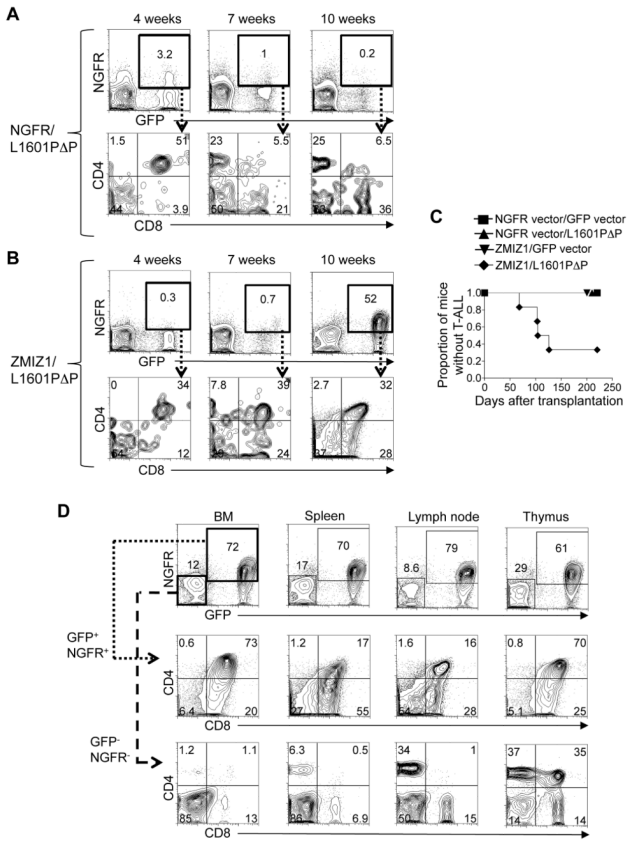

Figure 1. Ectopic expression of ZMIZ1 induces T-ALL in collaboration with NOTCH1

Mice were reconstituted with 5FU-treated donor BM cells after transduction with indicated retrovirus. Representative flow cytometric analysis of peripheral blood of a NGFR/L1601PΔP mouse (A) and a ZMIZ1/L1601PΔP mouse (B). (C) Kaplan-Meier curves showing the fraction of mice without T-ALL after bone marrow transplantation. 6–8 mice per group. (D) Representative flow cytometric analysis of CD4/CD8 expression of a ZMIZ1/L1601PΔP mouse with T-ALL. Negative, non-transduced controls are shown ($NGFR^-$ GFP^- cells).

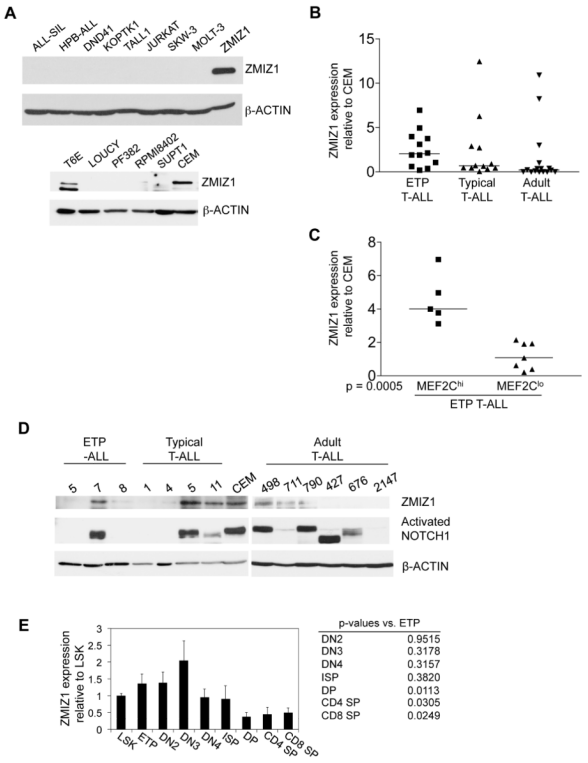

Figure 2. Expression of ZMIZ1 in T-ALL cell lines, primary T-ALL samples, and normal thymopoiesis

(A) 14 T-ALL cell lines were screened for ZMIZ1 expression by Western blot. ZMIZ1=positive control, 8946 cells transduced with ZMIZ1 and L1601PΔP retroviruses. (B, C) 12 primary pediatric human ETP-ALL samples, 12 primary pediatric human typical T-ALL samples, and 15 primary adult human T-ALL samples were screened for ZMIZ1 expression by qPCR. Expression is shown relative to the CEM cell line. The horizontal line shows median expression. In (C), the ETP-ALL samples were divided into samples having more or less MEF2C than CEM cells. (D) Primary human T-ALL samples were screened for ZMIZ1 and activated NOTCH1 expression by Western blot. Sizes of mutant NOTCH1 proteins vary depending on the sizes of the C-terminal PEST truncations. (E) Murine thymocytes were sorted and screened for Zmiz1 by qPCR. The expression is shown relative to LSK cells as means ± s.e.m.

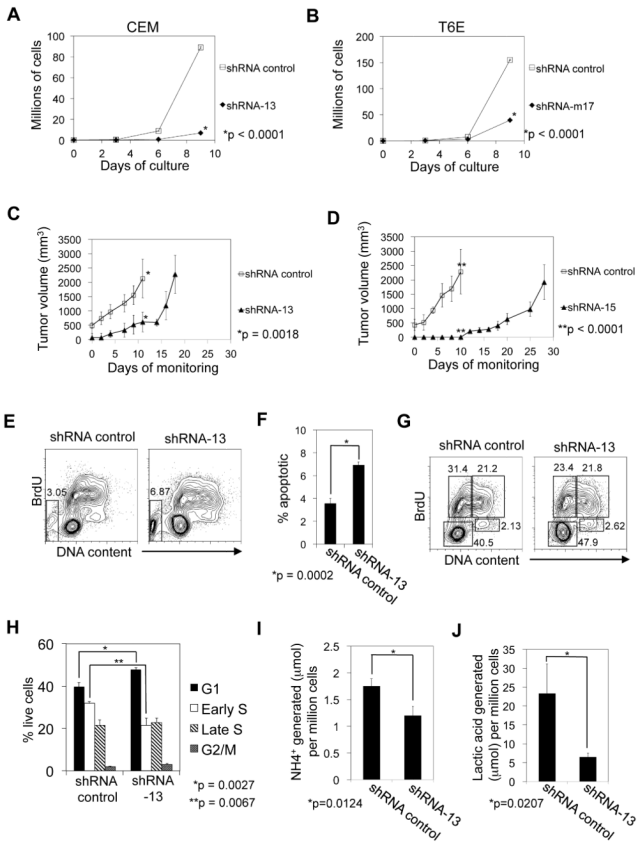

Figure 3. ZMIZ1 is a potential therapeutic target

(A) CEM cells were transduced with nonsilencing control shRNA or ZMIZ1-silencing shRNA-13. Extrapolated cell counts were determined by flow cytometry. (B) T6E cells were transduced with control shRNA or Zmiz1-silencing shRNA-m17 as in (A). CEM cells were transduced with ZMIZ1-silencing shRNA-13 (C) or shRNA-15 (D) and then injected into NOD-SCID-γ-chain deficient mice. *Mice were sacrificed. (E–J) Transduced CEM cells were pulsed with BrdU, and analyzed by flow cytometry. Apoptotic cells in the sub-2N gate are indicated in the box in (E) and graphed in (F). Non-apoptotic cells are shown in (G) and subdivided into various stages of cell cycle (H) – lower left box (G1); upper left box (early S); upper right box (late S); lower right box (G2/M). NH_4^+ (I) and lactic acid (J) in the supernatant was determined.

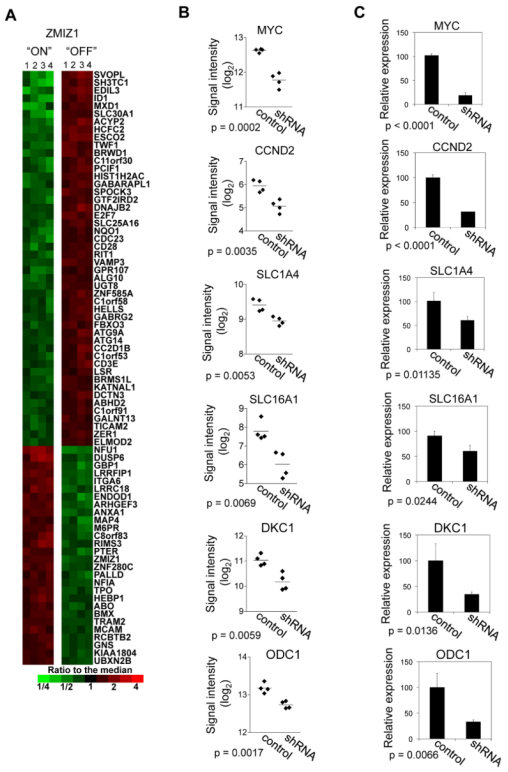

Figure 4. Identification of ZMIZ1-regulated genes in CEM cells

(A) Columns represent biological quadruplicate samples from CEM cells transduced with nonsilencing shRNA control or ZMIZ1-silencing shRNA-13. Human U133 Plus 2.0 GeneChips were used. Probe sets with $p<0.0005$ and fold-changes >2-fold are shown (53 up and 35 down probe sets). (B) Signal intensities of six C-MYC-related probe sets were compared. Horizontal lines indicate means. (C) Expression was validated by qPCR.

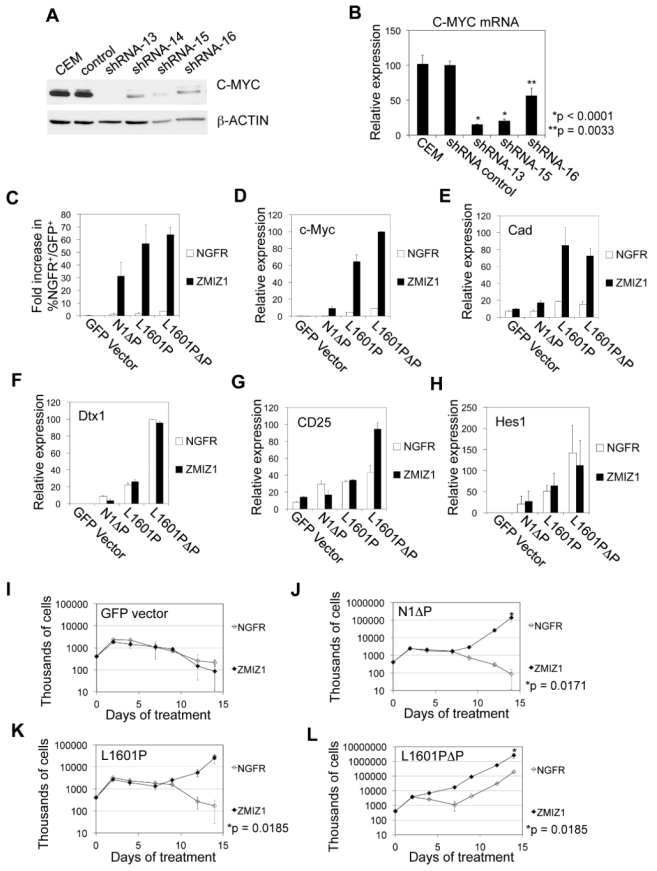

Figure 5. C-MYC is a target of ZMIZ1

CEM cells were transduced with ZMIZ1-silencing shRNA. C-MYC expression was measured by Western blot (A) and by qPCR (B) relative to the level in non-transduced cells. (C) 8946 cells were transduced with the NGFR empty vector (open columns) or ZMIZ1 (black columns) and with the indicated NOTCH1 alleles. After 6 days of doxycycline treatment, the %NGFR$^+$GFP$^+$ cells was measured by flow cytometry and divided by the starting percentage prior to treatment to derive the fold increase in %NGFR$^+$GFP$^+$ cells. (D–H) Sorted 8946 cells were analyzed for c-Myc (D), Cad (E), Dtx1 (F), CD25 (G), and Hes1 (H) by qPCR. Expression is presented as a percentage of the value in ZMIZ1/L1601PΔP-transduced cells. (I–L) Sorted 8946 cells were treated with doxycycline. Open symbols represent 8946 cells co-transduced with the empty NGFR vector. Closed symbols represent 8946 cells co-transduced with ZMIZ1.

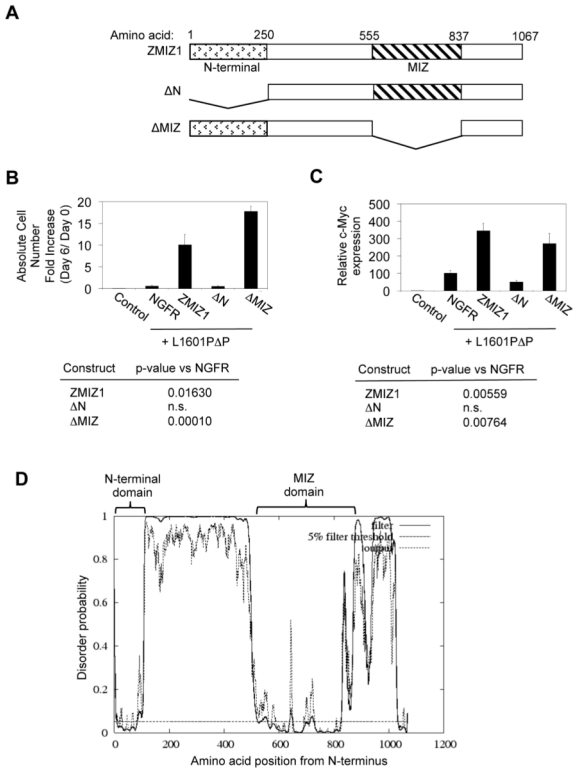

Figure 6. ZMIZ1 may regulate c-Myc through a novel MIZ-independent mechanism

(A) Schematic diagram of the mutants of ZMIZ1 used in this experiment. (B) 8946 cells were transduced with the indicated ZMIZ1 constructs in the NGFR vector with the activated NOTCH1 allele L1601PΔP. After 6 days of doxycycline treatment, the absolute number of $NGFR^+GFP^+$ cells was counted and divided by the starting number to derive the absolute cell number fold increase. (C) Sorted $NGFR^+GFP^+$ 8946 cells were analyzed for c-Myc by qPCR relative to the NGFR vector. Control=8946 cells transduced with MigR1 and NGFR vectors. (D) Disordered profile plot of ZMIZ1 generated by DISOPRED2 (http://bioinf.cs.ucl.ac.uk/disopred/).

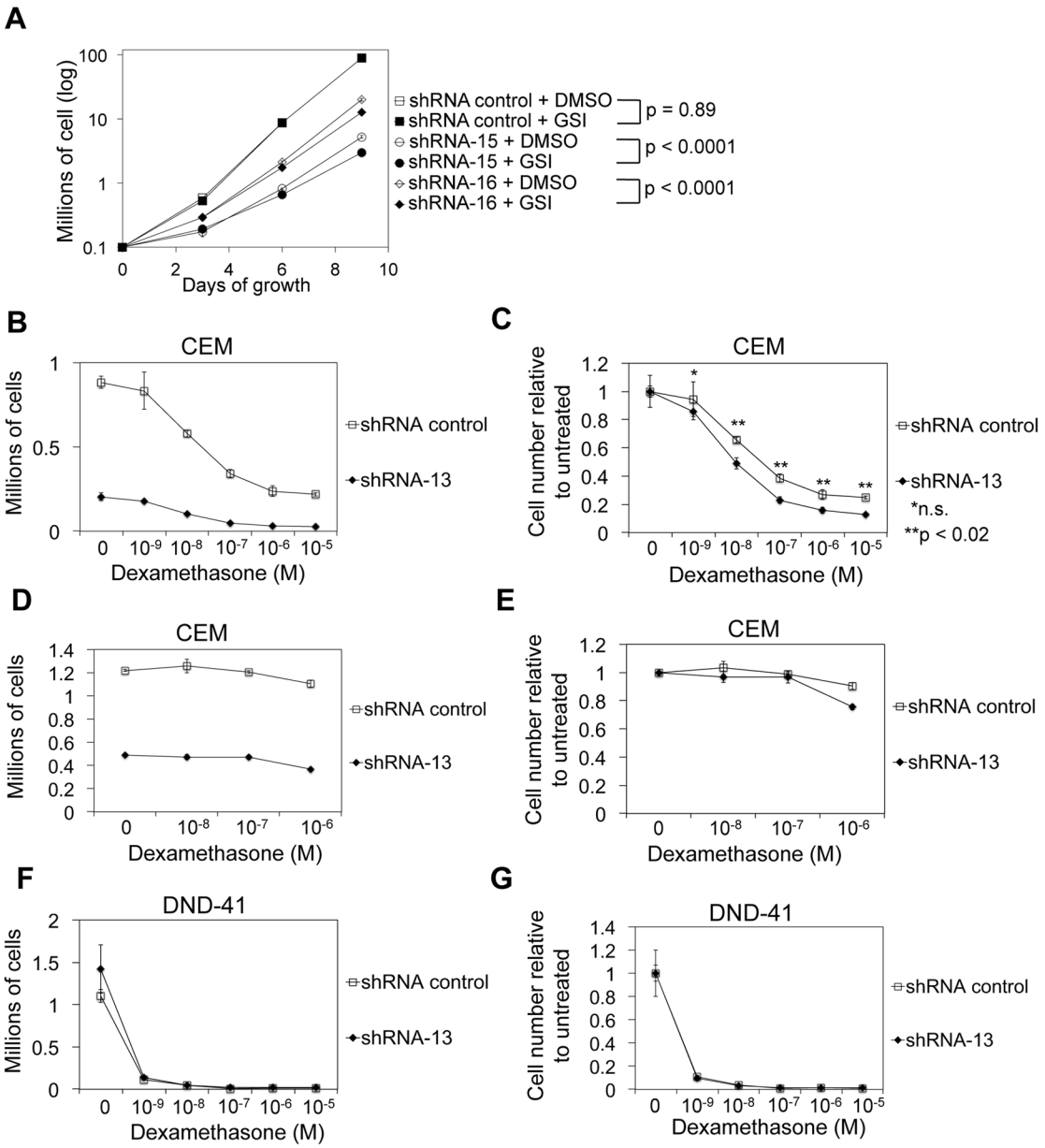

Figure 7. ZMIZ1 inhibition sensitizes leukemic cells to NOTCH inhibitors and glucocorticoids

(A) CEM cells were transduced with ZMIZ1-silencing shRNA and treated with DMSO or GSI. P<0.0001 for interaction tests using an ANOVA model of log-transformed data on Day 9 counts (B–C). Transduced CEM cells (80,000 cells/ml) were treated with dexamethasone and cultured (B). Relative cell number is shown in (C). P-values are derived from an ANOVA model with 12 means. (D–E) CEM cells were treated as in (B–C) in the presence of 1 mM mifepristone. (F–G) A similar experiment was performed as in (B–C), but using DND-41 cells. (B–G) Dexamethasone concentration is plotted on x-axis.